HAL open science

Effect of titanium dioxide film thickness on photocatalytic and bactericidal activities against Listeria monocytogenes

Marion Barthomeuf, Xavier Castel, Laurent Le Gendre, Justine Louis, Martine Denis, Christine Pissavin

To cite this version:

Marion Barthomeuf, Xavier Castel, Laurent Le Gendre, Justine Louis, Martine Denis, et al.. Effect of titanium dioxide film thickness on photocatalytic and bactericidal activities against Listeria monocytogenes. Photochemistry and Photobiology, 2019, 95 (4), pp.1035-1044. 10.1111/php.13078 . hal-01966652

HAL Id: hal-01966652

https://hal.science/hal-01966652v1

Submitted on 14 Jan 2019

HAL is a multi-disciplinary open access archive for the deposit and dissemination of scientific research documents, whether they are published or not. The documents may come from teaching and research institutions in France or abroad, or from public or private research centers.

L'archive ouverte pluridisciplinaire **HAL**, est destinée au dépôt et à la diffusion de documents scientifiques de niveau recherche, publiés ou non, émanant des établissements d'enseignement et de recherche français ou étrangers, des laboratoires publics ou privés.

Article type : Research Article

Accepted Article

Effect of titanium dioxide film thickness on photocatalytic and bactericidal activities against *Listeria monocytogenes*

Marion Barthomeuf[1], Xavier Castel[2], Laurent Le Gendre[2], Justine Louis[1], Martine Denis[3], Christine Pissavin*[1]

[1]. Univ Rennes, F-22000 Saint-Brieuc, France

[2]. Univ Rennes, CNRS, IETR – UMR 6164, F-22000 Saint-Brieuc, France

[3]. Anses – Laboratoire de Ploufragan-Plouzané / Unité Hygiène et Qualité des Produits Avicoles et Porcins, F-22440 Ploufragan, France

*Corresponding author e-mail: christine.pissavin@univ-rennes1.fr (Christine Pissavin)

ABSTRACT

Structural, microstructural and bactericidal surface properties of TiO_2-coated glass substrates elaborated by reactive RF-sputtering are investigated. As pathogenic bacteria in biofilms are a major concern in food industries due to their growing resistance to cleaning and sanitizing procedures, the development of photoactive surfaces exhibiting bactericidal properties is acknowledged as an

This article has been accepted for publication and undergone full peer review but has not been through the copyediting, typesetting, pagination and proofreading process, which may lead to differences between this version and the Version of Record.

effective approach to tackle bacterial contaminations. Our principal aim concerns the study of the photoactive top-layer thickness impact (from 80 nm to ~500 nm) on *Listeria monocytogenes*. Structural characterization of the TiO_2 layers demonstrates that anatase and rutile phases are both present, depending on the film thickness. Photocatalytic activity of the samples has been evaluated through the degradation of aqueous methylene blue (MB) solutions under UVA light illumination for various time periods. The results show an efficiency rating increase according to TiO_2 film thickness up to a threshold value close to 400 nm. Moreover a significant decrease of the adherent bacteria number is observed after 20 min of UVA illumination. The quantitative study of the bactericidal activity associated with scanning electron microscopy observations of the post-process bacteria damaged cells demonstrates the efficiency of the 240 nm-thick TiO_2 coating sample. The results are correlated with the production of hydroxyl radical during the process of photocatalysis.

INTRODUCTION

In food industry environments microbial, biofilms grown on work surfaces are the source of contamination, food-borne infections and also equipment damages (1, 2). Biofilms represent therefore a recurrent economic and food safety problem. It appears difficult to remove a biofilm once it is formed on food plant surfaces. Indeed the complex biofilm structure protects bacteria from classic disinfection and sanitizing procedures (3–7). Some bacteria, such as *Listeria monocytogenes*, can persist in various food plant environments from months to several years even when appropriate hygienic measures are applied (8, 9). Reis-Teixeira and coworkers have demonstrated that although *L. monocytogenes* is not able to form thick multilayer biofilms, the cells can persist on abiotic surfaces (10). This result confirms the need to focus on measures or techniques to avoid biofilm formation, instead of trying to fight against mature biofilms. Deposition of semiconductor materials in thin coatings is an efficient way of biologically active and self-sanitizing surface preparation. Antibacterial activity of such top-layers is photoinduced through the

.

Accepted Article

formation of reactive oxygen species (ROS) when irradiated by light energy higher than the band gap value (11). Among chemically stable, non-toxic and cost-effective materials, titanium dioxide (TiO_2) has been widely studied as semiconducting oxide for a large range of photocatalytic applications (12). TiO_2 material exhibits different polymorphic phases: anatase, rutile and brookite. Rutile is thermodynamically stable, while anatase and brookite phases are in metastable states (13). Among the three crystalline phases, anatase presents the highest photocatalytic and bactericidal activity (14, 15). When TiO_2 is irradiated by UV light, it produces pairs of electrons and holes. These either recombine, or migrate to the surface of the catalyst where they can participate in oxidation and reduction reactions by generating strong oxidative radicals (hydroxyl radicals, superoxide anions and hydrogen peroxide) that decompose organic compounds (16–18). Therefore, TiO_2 can be used as a photocatalytic antibacterial material: it combines chemical stability, biocompatibility and high potential for self-cleaning. That way, TiO_2-assisted photocatalytic disinfection, purification or clean-up processes have been evaluated on a wide range of organisms, including viruses, bacteria, fungi and algae (19–22).

Photocatalysts are conventionally available in powder form which makes the catalyst particles removal very difficult and expensive once work has been completed. This drawback can be overcome by immobilizing the catalyst onto or as a surface, at the expense of its developed corrugated surface (16, 23). TiO_2 photocatalytic coatings can be elaborated by various techniques, such as sol-gel process (24), chemical vapor deposition (25) and sputtering deposition methods (26). Radiofrequency (RF) and direct current (DC) sputtering are ones of the most available methods, frequently used in mass production due to their high deposition rates, high reliability, moderate running costs and possibility of covering a large range of substrate types (27).

.

Accepted Article

In this work, titanium dioxide thin films with various thicknesses were grown by RF magnetron sputtering technique on glass substrates to investigate the effect of the TiO_2 film thickness on the photocatalytic and bactericidal activities. Transparent substrates have been especially selected in the present study to extract the intrinsic optical characteristics of the photoactive coatings. The elaborated samples have been tested against the relevant food-born pathogen *L. monocytogenes*.

MATERIALS AND METHODS

Bacterial strain. Two strains of *L. monocytogenes* were considered in the present study: the *L. monocytogenes* ScottA reference strain (28) and the ECL 136 environmental strain sampled in a food plant (29). Each strain was stored at -70°C in Brain Heart Infusion (BHI) broth (Biokar, France) containing 40% (v/v) of glycerol. After the strain culture on Plate Count Agar (PCA) for 18 hours at 37°C, one colony was placed into BHI broth for 7 hours, as a pre-culture, at 37°C. Using the pre-culture, the appropriate broth was inoculated for an overnight sub-culture. After this, the bacterial suspension concentration was adjusted to 10^8 CFU/mL by measuring its optical density at 600 nm, and confirmed by enumeration on BHI. Then 50 µL of these suspensions have been loaded onto TiO_2 thin film to assess the susceptibility of the strains to UVA (365 nm) and to measure the bactericidal activity.

TiO_2 film elaboration. TiO_2 thin films were deposited on (50 mm × 50 mm × 0.7 mm) soda-lime glass substrates by RF magnetron sputtering technique (30, 31). The deposition chamber (Plassys MP 450S) that contained a titanium metal target (100.4 mm diameter, 99.995% purity) was pumped down to 5×10^{-5} Pa by a turbomolecular rotary pump system. The distance between the target and the substrate was set at 80 mm. Glass substrates were first cleaned in an alkaline lye at 60°C for 15 min, rinsed copiously with deionized water (10 min) and dried under a steam of dry nitrogen. The

.

Accepted Article

glass substrate, clamped on a sample holder, was then introduced in the deposition chamber via a loadlock chamber. The titanium target was supplied with RF power through an automatic matching network. Before each deposition step, the target was pre-sputtered in pure argon (Ar) atmosphere (2.75 Pa) under 50 W RF power for 10 min to remove any target surface contaminates. Then a mixture of argon (Ar) and oxygen (O_2) gas was bled into the sputtering chamber and adjusted by two mass flow controllers. The different parameters during TiO_2 deposition were set as follows: RF power: 200 W, substrate temperature: 440°C, O_2/Ar volume ratio: 3% and working pressure: 2.75 Pa. In order to obtain different film thicknesses, six deposition times: 60, 120, 180, 240, 300 and 360 min were used. The elaborated films are denoted in the present paper by TiO_2-film thickness, such as TiO_2-80nm (film thickness d = 80 nm and sputtering time = 60 min). After deposition, each sample was cleaved into coupons of 1cm×1cm each.

Physical characterizations of the TiO_2 thin films. A standard 4-point probe configuration, with a 225 Keithley current source and a 7050 Schlumberger microvoltmeter, provides the sheet resistance R_S at room temperature.

Optical transmittance was recorded by a UV–Visible spectrophotometer (Perkin Elmer Lambda 20 (Waltham, MA, USA), scanning speed 240 nm/min, 2 nm width slit) in the 200–1100 nm spectral range at normal incidence. The UV–Visible spectrophotometer was previously calibrated with air (blank). In region of strong absorption, the transmittance of the thin film T is expressed in terms of absorption coefficient α and film thickness d, as follows:

$$\ln(T) = -\alpha \times d$$

Taking into account the indirect-allowed transition of the TiO_2 band structure (32), the absorption coefficient is expressed by:

.

Accepted Article

$$(\alpha h\nu)^{1/2} = A\times(h\nu - Eg)$$

where $h\nu$ is the photon energy, A is a constant independent of photon energy and Eg is the optical band gap of TiO_2. By extrapolating the linear part of $(\alpha h\nu)^{1/2}$ versus energy, Eg value is determined for $(\alpha h\nu)^{1/2} = 0$ with an accuracy of 0.05eV (33).

X-Ray Diffraction (XRD) analyses were performed on a Seifert 3003 PTS diffractometer in θ–2θ mode. A parallel beam configuration was used with a Ge (220) monochromator mounted on the primary beam (Cu $\lambda_{K\alpha1}$ = 0.154056 nm). Data were recorded from 10° to 80° with a step angle of 0.01° and a scan rate of 0.15°/min. TiO_2 peak indexation has been performed in reference to the joint committee in powder diffraction standards files: 71-1167 for anatase phase and 77-0442 for TiO_2 rutile phase.

Surface and cross-section observations were conducted on a Jeol JSM-5600 Scanning Electron Microscope (SEM) operating at 10 kV. Thickness of the TiO_2 films was measured by SEM cross-sectional view on cleaved sections.

Photocatalytic activity of the TiO_2 coatings. Photocatalytic activity of the TiO_2 coated glass samples under UVA illumination was assessed by the methylene blue (MB) test (34) using a UVA lamp at 365 nm, 1350 µW/cm² (Vilbert Lourmat, VWR), for 60 minutes at a distance of 2 cm. Bare glass coupons have been used as negative controls.

Each coupon (coated with or without TiO_2 thin film) was placed into a well of a 24-well microplate (Greiner Bio-one, Austria) and loaded with 50 µL of a MB solution at 0.002% (w/v). After UVA illumination, 950 µL of saline water (9 g/L NaCl) was added in each well. Absorbance was measured with a visible spectrophotometer (Thermospectronic, Biomate3, France) at 650 nm. The decrease of the optical density before and after UVA illumination evidences the photocatalytic activity of the

.

Accepted Article

TiO_2 thin layers in comparison with negative controls. The photocatalytic activity PA is expressed as the ratio between the relative variation of the absorbance ($A-A_0$) and the initial absorbance A_0, as follows:

$$PA = 100\times(A-A_0)/A_0$$

Bactericidal activity of the TiO_2 coatings. For bactericidal activity measurements, coupons of glass (negative controls) and coupons coated with TiO_2 thin layers (1 cm^2 in size) were placed into wells of a 24-well microplate. Then 50 µL of the prepared bacterial suspension were loaded onto the surface of each coupon to obtain an initial load of 5×10^6 bacteria. All coupons were incubated at 20°C for 3 hours to provide bacterial adhesion. The incubation was done in a wet atmosphere to avoid any drying effect of the coupons. After the adhesion step, half of the coupons were exposed to UVA radiations (365 nm, 20 min, 2 cm distance between coupons and UVA lamp); the other coupons were placed in the dark.

The bactericidal activity of the TiO_2-coated samples was assessed by two different ways: by enumerating the surviving bacterial cells and by observing the morphology of the cells anchored on the coupon surface by SEM.

For the enumeration of the surviving bacterial cells, coupons with adherent cells were first washed twice with saline solution and placed in 2 mL of saline solution for sonication at 47 kHz for 20 min (Ultrasonic Bath 3210, Branson, USA) to take off adherent cells. Cultivable cells were then enumerated on BHI agar plates after 48 hours at 37°C.

The decadic logarithm of reduction, i.e. log (N/N_0) was computed, where N_0 is the number of bacteria deposited onto coupons expressed in CFU, and N is the number of cultivable bacteria after treatment expressed in CFU.

.

Accepted Article

For the morphology observation of the cells anchored on the coupon surface by SEM, coupons with adherent cells were immersed in a 3% glutaraldehyde solution prepared in 0.1M phosphate buffer for 1 hour to allow fixation of the cells. Then coupons were washed twice with saline water and immerged in successive ethanol baths with increasing percentage in vol.: 50%, 75% and 90% for 5 min each and ethanol at 100% for 30 min. Finally ethanol was replaced using a hexamethyldisilazane (HMDS) (Sigma-Aldrich, France) gradient at 50%, 75% in vol. for 10 min each and 100% for 30 min. HMDS is a drying agent and is used as a good alternative to Critical Point Drying for SEM sample preparation (35). At the end, the coupons were dried at room temperature for 24 hours for final SEM observation.

ROS detection. The detection of ROS was performed on coupons of bare glass (negative controls) and coupons coated with TiO_2 thin layers (1 cm² in size). The involvement of hydroxyl radicals $^{\bullet}OH$, has been underlined using the methylene blue degradation test adding mannitol, a scavenger of $^{\bullet}OH$. Coupons were placed into a 24-well microplate. 50µL of a solution of MB (0.002%) with a solution of 300 mM mannitol were added onto the surface of each coupon. After UVA illumination for 20 min, absorbance of the solution was determined in order to assess the involvement of $^{\bullet}OH$ in the photocatalysis reaction.

Statistical analysis. Statistical tests were carried out by using a two sample Student t-test with the same variance (XL Stats, free version, Addinsoft) and "R" software. Significant differences were indicated for each treatment ($p<0.05$).

.

Accepted Article

RESULTS

Characterization of the TiO_2 thin films

Six TiO_2 thin films have been elaborated by RF sputtering according to various deposition times (from 1 to 6 hours) with the same substrate temperature and partial pressure of oxygen in argon (Table 1). An average deposition rate of 1.33 nm/min was obtained with the sputtering parameters as reported in Table 1. The sheet resistance (R_S) of the samples, measured at room temperature, are beyond the measurement range of our setup ($R_S > 5\times10^9\ \Omega$/sq). Indeed TiO_2 thin film resistivity (ρ) is extremely high, $\rho > 10^6\ \Omega$.cm (36), leading for the highest thickness (d = 480 nm) to expected sheet resistance values higher than $2\times10^{10}\ \Omega$/sq. Those values put TiO_2 on the borderline between semiconductors and insulators.

The TiO_2 phases were identified by XRD. Figure 1 presents the XRD patterns according to the TiO_2 films thickness. On the one hand, a permanent signature of the anatase phase (main peak at 2θ = 25.271° that corresponds to the (101) orientation appears on all diffraction patterns. On the other hand, the rutile phase is observed on the thicker films (d higher than 240 nm). From a TiO_2 thickness of 400 nm, the contributions of the rutile and anatase phases on XRD patterns are qualitatively similar.

Figure 2 shows the surface morphology of the TiO_2 thin films observed by SEM according to the film thickness. SEM images exhibit uniform distribution of submicron-sized grains and are crack free.

To assess the optical properties of the TiO_2 films, optical transmission spectra of the samples have been recorded in air (data not shown) and the band gaps Eg have been computed. Eg values of the thinner films are slightly higher than that of the thicker films. On thin films, as the reported band-gap values of the pure anatase and rutile phases are in the range [3.3 - 3.2 eV] and [3.1 - 3.0 eV]

.

Accepted Article

respectively (32, 37-41), the decrease of the optical band gap versus the thickness supports the phase variation from anatase to rutile, as observed on the XRD patterns (Figure 1).

Photocatalytic properties of the TiO_2 coatings

The decrease of the methylene blue absorbance at 650 nm according to illumination time is presented in Figure 3. The six TiO_2 thin films exhibit a significant MB discoloration rate after 60 min of UVA illumination (Student test; $p<0.$) compared with both samples without UVA activation and the bare glass substrate (Figure 3A). An exponential decrease is observed and suggests first-order kinetics. According to the $-\ln(A/A_0)=kt$ equation, a straight line is fitted to the data and the apparent first-order constant k is retrieved from the slope (Figure 3B). As the TiO_2 thin film thickness increases, the MB discoloration rate increases too. The degradation rate saturates above the 400 nm film thickness value.

Bactericidal properties of the TiO_2 coatings

The antibacterial tests were carried out on the two strains of *L. monocytogenes* to determine the inactivation performance of the six TiO_2 coatings grown on glass substrates. The results of bactericidal assays, with and without UVA illumination, and using the bare glass substrate as negative control, are presented in Figure 4. The measurements undertaken on the bare glass substrate exhibit no significant bactericidal effect on both strains of *L. monocytogenes* in the dark and under UVA illumination (Figure 4).

.

Accepted Article

Without UVA radiation, the number of adherent cells is similar over all samples, on the bare glass coupons as well as on the TiO_2 coatings whatever their thickness. On both strains, the difference in the bacteria natural ability to survive on the bare glass substrate, with or without UVA illumination, is not significant (Student test, $p>0.05$). The bacteria adhesion on the coupons is not any more affected by the TiO_2 coatings, as shown by the measurements in the dark (Figure 4).

After photoactivation with UVA radiations for 20 min, TiO_2 coatings as a whole provide a strong bactericidal effect on both strains. On *L. monocytogenes* ScottA (Figure 4 A), the number of adherent bacteria decreases gradually with the increase of the TiO_2 thickness. That way, a reduction in the number of surviving cells of 2.5 log is obtained with the 480 nm-thick TiO_2 coating. On *L. monocytogenes* ECL136 (Figure 4 B), the photocatalytic efficiency of the active coating increases from the first few tens of nanometer and reaches a saturation point with a TiO_2 thickness close to 240 nm, corresponding to a similar efficiency (2.5 log) measured on the previous reference strain with the thicker TiO_2 coating ($d \approx 500$ nm) (Figure 5).

The cells of both strains, environmental and reference strains adhering onto the TiO_2-240 nm coupon surface and onto the bare glass surface were exposed to UVA radiations for 20 min and were observed by SEM. Damaged cells occur on the functionalized surface after UVA activation, by contrast to those adhering on the bare glass coupons and showing no apparent morphological damages (Figure 6). Damaged cells appear empty without cytoplasmic content as “ghost cells”, with some membranes drilled. Indeed, UVA illumination could be responsible for DNA mutation and death cell if UV exposure is long. In our case, we used UVA wavelength, the less damaging UV rays (λ = 365 nm) for a maximum time of 20 min.

All these observations have been correlated with the results of ROS detection. The involvement of $^{\bullet}OH$ in methylene blue degradation has been confirmed with the TiO_2-240 nm sample (Figure 7). After UVA illumination, TiO_2 coupons exhibit a MB discoloration. When mannitol is added to the MB

.

Accepted Article

solution, no MB discoloration has been observed. The absorbance spectra of the MB solution after UVA illumination was the same as the absorbance observed with the bare glass coupons, showing that $^{\bullet}OH$ scavenger presence has enabled to achieve the absorbance of the negative control.

DISCUSSION

In the present study, glass substrates have been functionalized by RF sputtering deposition of TiO_2 thin films. Influence of the TiO_2 thickness on the photocatalytic and bactericidal activities has been investigated. Thin layers have been obtained from deposition time of 1 hour up to 6 hours, and thickness is linearly correlated to deposition time with TiO_2 thin layers varying from 80 nm to 480 nm respectively. The deposition rate of 80 nm per hour is currently observed when using RF magnetron sputtering deposition for TiO_2 thin films (42). As the film thickness increases, the surface morphology changes. Heikkilä and co-workers, in 2009, concluded that grains and surface roughness increase toward the TiO_2 film thickness (23).

Using our sputtering parameters, TiO_2 thin films exhibit an anatase structure at low thicknesses (d thinner than ~240 nm) whereas the crystalline phase evolves toward a combination of anatase and rutile structures with the thicker films. Such dual structure could help to achieve a better efficiency in bactericidal activity. Indeed many studies have previously underlined a higher photocatalytic performance in a wide range of applications (self-cleaning surfaces, air and water purification, H_2 production by water splitting…) when TiO_2 provides a mixture of anatase and rutile structures (43) at a specific [anatase : rutile] ratio in the range [70 : 30 – 80 : 20] respectively, as found in the commercially available titania photocatalyst Degussa P25 (14, 15, 44). In that case, the efficiency of the UV-driven organic pollutants photocatalytic oxidation is enhanced by the existence of nanoscale

.

Accepted Article

heterojunctions between the anatase and the rutile phases (45-46). In this context, on powder or on mesoporous nanofibers, those multi-semiconductor/semiconductor junctions between the TiO_2 polymorphs modify the band-gap structure and consequently the photocatalytic activity of the material. Concerning the bactericidal performance under UV light, while anatase-type TiO_2 powders or thin films always exhibit an antibacterial activity on various types of bacteria (47–50), rutile-type titanium dioxide phase demonstrates no bactericidal activity (15, 16, 48, 51) unless the film is fully {111}-oriented (52). Conversely, under the visible light, while the detrimental effect of the anatase phase on the survival of the bacteria is non-existent (53) or limited (54), the rutile structure takes over the activity (53–55). As the rutile phase exhibits a lower band-gap value than that of the anatase, its ability to use the blue part of the visible spectrum explains in part this behaviour. Moreover, ROS types, natures and quantities depend on both titanium dioxide structure and radiation wavelengths. That way, it has been shown that under UV illumination, the activity of anatase materials is primarily related to the efficient production of •OH species (56) while visible light illumination largely enhances $\bullet O_2^-$ formation on rutile surfaces (51, 56). One must also keep in mind that the exact composition of the ROS mixture formed as well as its reactivity depends not only on the structure and texture of the photocatalyst, but also on the bacteria-type itself. In the present study, TiO_2 coatings thicker than 240 nm, composed of anatase and rutile phases, exhibit the best photocatalytic and bactericidal activities. The kinetic data retrieved from the photocatalytic degradation of MB can be correlated with the bactericidal performance. The photocatalytic activity of our TiO_2 coatings with thicknesses up to 400 nm, allowed more than 90% of MB discoloration in one hour. Commercial Degussa P25®, tested by Barnes and co-workers in 2013, provided 76% of discoloration rate after one hour exposure under UVA radiations at 365 nm (57). Moreover Heikkilä and co-workers also grew TiO_2 thin films by Atomic Layer Deposition (ALD) technique (23). Their anatase-TiO_2 films with various thicknesses (from 50 to 520 nm) caused MB discoloration, around 10% after 1 hour-UVA irradiation. As we observed above, Heikkilä and co-workers showed an exponential decrease which suggests first-order kinectics. Initial MB concentration, temperature,

.

Accepted Article

TiO_2 concentration and form, illumination wavelength have been shown to influence the photocatalytic activity and especially the kinetics rate (58). Comparison of kinetics rate is therefore difficult because of the spread in the initial settings.

TiO_2 photocatalysts as fine particles have already been studied to fight against bacteria in various environments such as medical environments (59-60), water disinfection field (61–64) or food plants (19, 20). However, the use of TiO_2 suspension presents a disadvantage in the postcatalytic catalyst removal (17, 65). In food plants, an alternative way concerns the development of stable coatings through thin film deposition. In the present work, RF magnetron sputtering technique has been used to grow TiO_2 thin films with different thicknesses. This type of functionalized materials aims to restrict the first step of biofilm formation by preventing the bacteria adhesion. For this purpose, the TiO_2 thin films have been tested against adherent *L. monocytogenes* bacteria and not against mature biofilms (19, 66). Unfortunately, these TiO_2 coatings do not provide any anti-adhesive property, since no difference has been observed between the number of bacteria grown on the bare glass substrates and those grown on the TiO_2 coatings without UVA illumination. Similarly Chorianopoulos and co-workers did not obtain any anti-adhesive effect on the *L. monocytogenes* ScottA bacteria grown onto glass coated with TiO_2 layers, without UVA irradiation (19).

After UVA activation of the TiO_2 layers, the surfaces present a strong bactericidal activity against both *L. monocytogenes* strains. This bactericidal effect can be related to the thickness of the TiO_2 layer and also to the TiO_2 crystalline phase as depicted in Figure 5. Indeed the presence of the rutile phase in addition to the anatase one in TiO_2 films thicker than 240 nm seems to be linked to the saturation effect undergone by the environmental strain *L. monocytogenes* ECL136.

.

Accepted Article

Active species (ROS) are produced by the photocatalytic TiO_2 coating. Concerning our TiO_2 coupons, hydroxyl radical production may be involved in the bactericidal activity. The use of mannitol as a scavenger highlighted the $^{\bullet}OH$ involvement in the MB discoloration, and thus in the photocatalytic activity. Other detection methods such as electron spin resonance observation, direct fluorescence or chemiluminescence exist. These methods are quantitative and accurate. However these methods require specific and expensive equipments to be performed (18). ROS as $^{\bullet}OH$ affect the cell wall integrity as observed by SEM, while direct UVA radiations do not affect their cell morphology. Indeed UV radiations may damage DNA and cause mutations (67). UV resistance of bacteria differs between species and also depends on the age of organisms, growth stage and also bacterial form (biofilm or adherent cells) (31, 68, 69). In general, Gram-positive bacteria tend to be more resistant to UV radiations than Gram-negative bacteria (31, 67).

Listeria monocytogenes ScottA and ECL136 belong to the serotypes 4b and 1/2a, respectively. The observed differences in susceptibility may be related to variable responses to oxidative stress as it was highlighted in a recent study (70). Moreover the composition of the teichoic acids is different between 4b and 1/2a serotype (71, 72). The wall components are known to be a target of the ROS generated by the TiO_2. Consequently this may contribute to the difference in susceptibility of the two *Listeria* strains

In conclusion, TiO_2 coatings deposited by RF sputtering technique on glass substrates and activated by UVA illumination exhibit bactericidal activity against the foodborne pathogen *L. monocytogenes*. Indeed a significant reduction of the adherent cells after 20 min of UVA exposure has been measured. 240 nm-thick TiO_2 coating is sufficient to promote optimal bactericidal activity against *L. monocytogenes* ECL316 whereas thicker films (~500 nm) are needed against *L. monocytogenes* ScottA. The TiO_2 surface functionalization paves the way to improve cleanability and disinfection in .

Accepted Article

food industry environments. Work is under progress to grow such TiO_2 thin films onto stainless steel substrates in order to be applied in food plants.

ACKNOWLEDGEMENTS

This work was supported by the European Union through the European Regional Development Fund (ERDF), and by the Ministry of Higher Education and Research, the French region of Brittany, through the CPER Projects 2015-2020 MATECOM and SOPHIE/STIC & Ondes. This work was also supported by a grant from Saint-Brieuc Armor Agglomération and the Département des Côtes d'Armor. We thank Stéphanie Bougeard for her help in statistical analysis, Maël Visdeloup and Nyedna Policarpo for their technical support.

REFERENCES

1. Trachoo N. 2003. Biofilms and the food industry. *Songklanakarin J. Sci. Technol*. 25(6):807–815

2. Abdallah M, Benoliel C, Drider D, Dhulster P, Chihib N-E. 2014. Biofilm formation and persistence on abiotic surfaces in the context of food and medical environments. *Arch. Microbiol*. 196(7):453–472

3. Gil MI, Selma MV, López-Gálvez F, Allende A. 2009. Fresh-cut product sanitation and wash water disinfection: problems and solutions. *Int. J. Food Microbiol*. 134(1–2):37–45

.

Accepted Article

4. Ibusquiza PS, Herrera JJR, Cabo ML. 2011. Resistance to benzalkonium chloride, peracetic acid and nisin during formation of mature biofilms by *Listeria monocytogenes*. *Food Microbiol*. 28(3):418–425

5. Soumet C, Méheust D, Pissavin C, Le Grandois P, Frémaux B, Feurer C, Le Roux A, Denis M, Maris P. 2016. Reduced susceptibilities to biocides and resistance to antibiotics in food-associated bacteria following exposure to quaternary ammonium compounds. *J. Appl. Microbiol*. 121(5):1275–1281

6. Colagiorgi A, Di Ciccio P, Zanardi E, Ghidini S, Ianieri A. 2016. A Look inside the *Listeria monocytogenes* biofilms extracellular matrix. *Microorganisms*. 4(3):1-12

7. Pilchova T, Hernould M, Prévost H, Demnerova K, Pazlarova J, Tresse O. 2014. Influence of food processing environments on structure initiation of static biofilm of *Listeria monocytogenes*. *Food Control*. 35:366–372

8. Bridier A, Sanchez-Vizuete P, Guilbaud M, Piard J-C, Naïtali M, Briandet R. 2015. Biofilm-associated persistence of food-borne pathogens. *Spec. Issue Predict. Model. Food*. 45, *Part B*:167–178

9. Carpentier B, Cerf O. 1993. Biofilms and their consequences, with particular reference to hygiene in the food industry. *J Appl Bacteriol*. 75(6):499–511

10. Reis-Teixeira FB, Alves VF, de Martinis ECP. 2017. Growth, viability and architecture of biofilms of *Listeria monocytogenes* formed on abiotic surfaces. *Braz. J. Microbiol*.48(3) :587–591.

11. Joost U, Juganson K, Visnapuu M, Mortimer M, Kahru A, Nõmmiste E, Joost U, Kisand V, Ivask A. 2015. Photocatalytic antibacterial activity of nano-TiO_2 (anatase)-based thin films: Effects on *Escherichia coli* cells and fatty acids. *J. Photochem. Photobiol. B*. 142(Supplement C):178–185

.

Accepted Article

12. Nakata K, Fujishima A. 2012. TiO_2 photocatalysis: Design and applications. *J. Photochem. Photobiol. C Photochem. Rev*. 13:169–189

13. Gopal M, Chan WJM, Jonghe LCD. 1997. Room temperature synthesis of crystalline metal oxides. *J. Mater. Sci*. 32(22):6001–6008

14. Navabpour P, Cooke K, Sun H. 2017. Photocatalytic properties of doped TiO_2 coatings deposited using reactive magnetron sputtering. *Coatings*. 7(1):433–449

15. Sirimahachai U, Phongpaichit S, Wongnawa S. 2009. Evaluation of bactericidal activity of TiO_2 photocatalysts: a comparative study of laboratory-made and commercial TiO_2 samples. *Songklanakarin J. Sci. Technol.* 31(5):517–525

16. Miao L, Tanemura S, Kondo Y, Iwata M, Toh S, Kaneko K. 2004. Microstructure and bactericidal ability of photocatalytic TiO_2 thin films prepared by RF helicon magnetron sputtering. *Appl. Surf. Sci.* 238(1–4):125–131

17. Ede S, Hafner L, Dunlop P, Byrne J, Will G. 2012. Photocatalytic disinfection of bacterial pollutants using suspended and immobilized TiO_2 powders. *Photochem. Photobiol*. 88(3):728–735

18. Nosaka Y, Nosaka AY. 2017. Generation and detection of reactive oxygen species in photocatalysis. *Chem. Rev*. 117(17):11302–11336

19. Chorianopoulos NG, Tsoukleris DS, Panagou EZ, Falaras P, Nychas GJ. 2011. Use of titanium dioxide (TiO_2) photocatalysts as alternative means for *Listeria monocytogenes* biofilm disinfection in food processing. *Food Microbiol*. 28(1):164–170

20. Kim B, Kim D, Cho D, Cho S. 2003. Bactericidal effect of TiO_2 photocatalyst on selected food-borne pathogenic bacteria. *Chemosphere*. 52(1):277–281

Accepted Article

.

21. Thabet S, Weiss-Gayet M, Dappozze F, Cotton P, Guillard C. 2013. Photocatalysis on yeast cells: toward targets and mechanisms. *Appl. Catal. B Environ*. 140–141:169–78

22. Gogniat G, Thyssen M, Denis M, Pulgarin C, Dukan S. 2006. The bactericidal effect of TiO_2 photocatalysis involves adsorption onto catalyst and the loss of membrane integrity. *FEMS Microbiol. Lett*. 258(1):18–24

23. Heikkilä M, Puukilainen E, Ritala M, Leskelä M. 2009. Effect of thickness of ALD grown TiO_2 films on photoelectrocatalysis. *J. Photochem. Photobiol. Chem*. 204(2–3):200–208

24. Calabria A. J, Vasconcelos WL, Daniel DJ, Chater R, McPhail D, Boccaccini AR. 2010. Synthesis of sol–gel titania bactericide coatings on adobe brick. *Constr. Build. Mater*. 24(3):384–389

25. Bessergenev VG, Mateus MC, Morgado IM, Hantusch M, Burkel E. 2017. Photocatalytic reactor, CVD technology of its preparation and water purification from pharmaceutical drugs and agricultural pesticides. *Chem. Eng. J.* 312(Supplement C):306–316

26. Singh J, Khan SA, Shah J, Kotnala RK, Mohapatra S. 2017. Nanostructured TiO_2 thin films prepared by RF magnetron sputtering for photocatalytic applications. *Appl. Surf. Sci*. 422(Supplement C):953–961

27. Ferraris S, Perero S. 2016. 2 - Smart and composite inorganic coatings obtained by sputtering: a promising solution for numerous application fields. *Smart Composite Coatings and Membranes*, ed MF Montemor, pp. 33–60. Woodhead Publishing

28. Fleming DW, Cochi SL, MacDonald KL, Brondum J, Hayes PS, Plikaytis B, Holmes M, Audurier A, Broome C, Reingold A.1985. Pasteurized milk as a vehicle of infection in an outbreak of Listeriosis. *N. Engl. J. Med*. 312(7):404–407

.

Accepted Article

29. Chasseignaux E, Gérault P, Toquin M-T, Salvat G, Colin P, Ermel G. 2002. Ecology of *Listeria monocytogenes* in the environment of raw poultry meat and raw pork meat processing plants. *FEMS Microbiol. Lett*. 210(2):271–275

30. Le Paven C, Le Gendre L, Benzerga R, Cheviré F, Tessier F, Jacq S, Traoré-Mantion S, Sharaiha A. 2015. Growth of (Sr,La)-(Ta,Ti)-O-N perovskite oxide and oxynitride films by radiofrequency magnetron sputtering: Influence of the reactive atmosphere on the film structure. *J. Cryst. Growth*. 413:5–11

31. Barthomeuf M, Raymond P, Policarpo N, Castel X, Le Gendre L, Denis M, Pissavin C. 2017. Bactericidal efficiency of UVA-active titanium dioxide thin layers on bacteria from food industry environments. *Mater. Technol. Adv. Perform. Mater*. 32(13): 782–791

32. Tang H, Prasad K, Sanjinès R, Schmid PE, Lévy F. 1994. Electrical and optical properties of TiO_2 anatase thin films. *J. Appl. Phys*. 75:2042–2047

33. Barka-Bouaifel F, Makaoui K, Jouan P-Y, Castel X, Bezzi N, Boukherroub R, Szunerits S. 2012. Preparation and photocatalytic properties of quartz/gold nanostructures/TiO_2 lamellar structures. *RSC Adv*. 2(32):12482–12488

34. Fu P, Luan Y, Dai X. 2004. Preparation of activated carbon fibers supported TiO_2 photocatalyst and evaluation of its photocatalytic reactivity. *J. Mol. Catal. - Chem*. 221(1):81–88

35. Hazrin-Chong NH, Manefield M. 2012. An alternative SEM drying method using hexamethyldisilazane (HMDS) for microbial cell attachment studies on sub-bituminous coal. *J. Microbiol. Methods*. 90(2):96–99

36. Casoti D, Orsini V, di Bona A, Gardonio S, Fanetti M, Valant M, Valeri S. 2018. Ageing effects on electrical resistivity of Nb-doped TiO_2 thin films deposited at a high rate by reactive DC magnetron sputtering. *Appl. Surf. Sci.* 455:267-275

.

Accepted Article

Accepted Article

37. Aarik J, Aidla A, Kiisler A-A, Uustare T, Sammelselg V. 1997. Effect of crystal structure on optical properties of TiO_2 films grown by atomic layer deposition. *Thin Solid Films*. 305(1):270–273

38. Daude N, Gout C, Jouanin C. 1977. Electronic band structure of titanium dioxide. *Phys. Rev. B*. 15(6):3229–3235

39. Camps E, Castrejon-Sanchez VH, Camacho-Lopez M, Basurto R. 2015. Influence of the nitriding process on the band-gap of TiO_2 thin films with phase mixture. *Thin Solid Films*. 581:54-58

40. Long H, Chen A, Yang G, Li Y, Lu P. 2009. Third-order optical nonlinearities in anatase and rutile TiO_2 thin films. *Thin Solid Films*. 517(19):5601-5604.

41. Liu HY, Huang RC. 2018. A study of anatase TiO_2-based thin film phototransitors by non-vacuum thin film deposition method. *IEEE Trans. Electron Devices*. 65(6):2517-2524

42. Nair PB, Justinvictor VB, Daniel GP, Joy K, James Raju KC, Devraj K, Thomas P. 2014. Optical parameters induced by phase transformation in RF magnetron sputtered TiO_2 nanostructured thin films. *Prog. Nat. Sci. Mater. Int*. 24(3):218–225

43. Yuangpho N, Le STT, Treerujiraphapong T, Khanitchaidecha W, Nakaruk A. 2015. Enhanced photocatalytic performance of TiO_2 particles via effect of anatase–rutile ratio. *Phys. E Low-Dimens. Syst. Nanostructures*. 67(Supplement C):18–22

44. Van der Meulen T, Mattson A, Österlund L. 2007. A comparative study of the photocatalytic oxidation of propane on anatase, rutile, and mixed-phase anatase–rutile TiO_2 nanoparticles: Role of surface intermediates. *J. Catal*. 251(1):131–144

45 Ghosh M, Lohrasbi M, Chuang SSC, Jana SC. 2016. Mesoporous titanium dioxide nanofibers with a significantly enhanced photocatalytic activity. *Chem. Cat. Chem*. 8:2525-2535

46 Bickley RI, Gonzalez-Carreno T, Lees JS, Palmisano L, Tilley RJD. 1991. A structural

.

investigation of titanium dioxide photocatalysts. *J. Solid State Chem.* 92:178-190

47. Cheng TC, Yao KS, Yeh N, Chang CI, Hsu HC, Gonzales F, Chang CY. 2011. Bactericidal effect of blue LED light irradiated TiO_2/Fe_3O_4 particles on fish pathogen in seawater. *Thin Solid Films*. 519(15):5002–5006

48. Joo H-C, Lim Y-J, Kim M-J, Kwon H-B, Han J-H. 2010. Characterization on titanium surfaces and its effect on photocatalytic bactericidal activity. *Appl. Surf. Sci*. 257(3):741–746

49. Sisti L, Cruciani L, Totaro G, Vannini M, Berti C, Tobaldi DM, Tucci A, Aloisio I, Di Gioia D, Commereuc S. 2012. TiO_2 deposition on the surface of activated fluoropolymer substrate. *Thin Solid Films*. 520:2824–2828

50. Lee HU, Lee SC, Lee SM, Lee JW, Kim HJ, Lee J. 2013. Improved photocatalytic and antibacterial activities of three-dimensional polycrystalline anatase TiO_2 photocatalysts. *Appl. Catal. Gen*. 467:394–99

51. Perelshtein I, Applerot G, Perkas N, Grinblat J, Gedanken A. 2012. A one-step process for the antimicrobial finishing of textiles with crystalline TiO_2 nanoparticles. *Chem. Weinh. Bergstr. Ger*. 18(15):4575–4582

52. Liu X, Zhang H, Liu C, Chen J, Li G, An T, Wong PK, Zhao H. 2014. UV and visible light photoelectrocatalytic bactericidal performance of 100% {111} faceted rutile TiO_2 photoanode. *Catal. Today*. 224:77–82

53. Veréb G, Manczinger L, Bozsó G, Sienkiewicz A, Forró L, Mogyorosi K, Hernadi K, Dombi A. 2013. Comparison of the photocatalytic efficiencies of bare and doped rutile and anatase TiO_2 photocatalysts under visible light for phenol degradation and *E. coli* inactivation. *Appl. Catal. B Environ*. 129:566–574

.

Accepted Article

54. Rincon AG, Pulgarin C. 2003. Photocatalytical inactivation of *E. coli*: effect of (continuous-intermittent) light intensity and of (suspended-fixed) TiO_2 concentration. *Appl. Catal. B-Environ*. 44(3):263–284

55. Kim C-H, Lee E-S, Kang S-M, de Josselin de Jong E, Kim B-I. 2017. Bactericidal effect of the photocatalystic reaction of titanium dioxide using visible wavelengths on *Streptococcus mutans* biofilm. Photodiagnosis *Photodyn. Ther*. 18:279–283

56. Zoltan T, Rosales MC, Yadarola C. 2016. Reactive oxygen species quantification and their correlation with the photocatalytic activity of TiO_2 (anatase and rutile) sensitized with asymmetric porphyrins. *J. Environ. Chem. Eng*. 4(4):3967–3980

57. Barnes RJ, Molina R, Xu J, Dobson PJ, Thompson IP. 2013. Comparison of TiO_2 and ZnO nanoparticles for photocatalytic degradation of methylene blue and the correlated inactivation of gram-positive and gram-negative bacteria. *J. Nanoparticle Res*. 15(2):1–11

58. Wu C-H, Chern J-M. 2006. Kinetics of photocatalytic decomposition of methylene blue. *Ind. Eng. Chem. Res*. 45(19):6450–6457

59. Campoccia D, Montanaro L, Arciola CR. 2013. A review of the biomaterials technologies for infection-resistant surfaces. *Biomaterials*. 34(34):8533–8554

60. Yoshinari M, Oda Y, Kato T, Okuda K. 2001. Influence of surface modifications to titanium on antibacterial activity in vitro. *Biomaterials*. 22(14):2043–2048

61. Claro EMT, Bidoia ED, de Moraes PB. 2016. A high-performance doped photocatalysts for inactivation of total coliforms in superficial waters using different sources of radiation. *J. Environ. Manage*. 177:264–270

.

Accepted Article

62. Fisher MB, Keane DA, Fernández-Ibáñez P, Colreavy J, Hinder SJ, McGuigan KG, Pillai SC, 2013. Nitrogen and copper doped solar light active TiO_2 photocatalysts for water decontamination. *Appl. Catal. B Environ*. 130–131:8–13

63. Kaan CC, Aziz AA, Ibrahim S, Matheswaran M, Saravanan P. 2012. Heterogeneous photocatalytic oxidation an effective tool for wastewater treatment – A review. *Studies on Wat. Manag. Issues, InTech*, 219–236

64. Robertson JMC, J. Robertson PK, Lawton LA. 2005. A comparison of the effectiveness of TiO_2 photocatalysis and UVA photolysis for the destruction of three pathogenic micro-organisms. *J. Photochem. Photobiol. Chem*. 175(1):51–56

65. Guillard C, Kartheuser B, Lacombe S. 2011. La photocatalyse : dépollution de l'eau ou de l'air et matériaux autonettoyants. *Tech. Ing. Génie Procédés Prot. Environ*. Base documentaire : TIB327DUO.

66. Carré G, Hamon E, Ennahar S, Estner M, Lett M-C, Horvatovich P,Gies JP, Keller V, Keller N, and Andre P. 2014. TiO_2 Photocatalysis damages lipids and proteins in *Escherichia coli*. *Appl. Environ. Microbiol*. 80(8):2573–2581

67. Gailunas KM, Matak KE, Boyer RR, Alvarado CZ, Williams RC, Sumner SS. 2008. Use of UV light for the inactivation of *Listeria monocytogenes* and lactic acid bacteria species in recirculated chill brines. *J. Food Prot*. 71(3):629–633

68. Bonsaglia ECR, Silva NCC, Fernades Júnior A, Araújo Júnior JP, Tsunemi MH, Rall VLM. 2014. Production of biofilm by *Listeria monocytogenes* in different materials and temperatures. *Food Control*. 35(1):386–391

Accepted Article

.

69. Vázquez-Sánchez D, Cabo ML, Ibusquiza PS, Rodríguez-Herrera JJ. 2014. Biofilm-forming ability and resistance to industrial disinfectants of *Staphylococcus aureus* isolated from fishery products. *Food Control*. 39:8–16

70 Huang Y, Morvay AA, Shi X, Suo Y, Shi C, Knøchel S. 2018. Comparison of oxidative stress response and biofilm formation of *Listeria monocytogenes* serotypes 4b and 1/2a. *Food Control.* 85:416–422

71. Fiedler F, Seger J, Schrettenbrunner A, Seeliger HPR. 1984. The biochemistry of murein and cell wall teichoic acids in the genus *Listeria*. *Syst. Appl. Microbiol*. 5:360–376.

72 Promadej N, Fiedler F, Cossart P, Dramsi S, Kathariou S, 1999. Cell wall teichoic acid glycosylation in *Listeria monocytogenes* Serotype 4b requires *gtcA*, a novel serogroup-specific gene. *J. Bacteriol*. 181:418–425.

FIGURE CAPTIONS

Figure 1. X-ray diffraction patterns of a) Bare glass substrate; b) TiO_2-80nm; c) TiO_2-170nm; d) TiO_2-240nm; e) TiO_2-310nm; f) TiO_2-400nm; g) TiO_2-480nm. (●) indicates anatase peaks and (*) indicates rutile peaks.

Figure 2. Surface morphology of the TiO_2 thin films observed by Scanning Electron Microscopy (×20 000): (A) TiO_2-80nm; (B) TiO_2-170nm; (C) TiO_2-240nm; (D) TiO_2-310nm; (E) TiO_2-400nm; (F) TiO_2-480nm.

.

Accepted Article

Figure 3. TiO_2 film thickness effect on the photocatalytic discoloration of methylene blue. A) Absorbance of the methylene blue is related to the initial value according to UVA irradiation time. B) Logarithm of the absorbance ratio of methylene blue. First order linear kinetics. The value is a mean of 3 measurements. Bare glass substrate (♦); TiO_2-80nm (■); TiO_2-170nm (▲); TiO_2-240nm (×); TiO_2-310nm (Δ); TiO_2-400nm (⊘; TiO_2-480nm (⇳.

Figure 4. Influence of the TiO_2 coatings and UVA illumination on cell viability of 2 bacterial strains A) *L. monocytogenes* ScottA; B) *L. monocytogenes* ECL136. Surviving cells are numerated on agar plates, N_0 is the cell number deposited onto the coupon and N is the number of surviving cells after 3 hours and subsequent irradiation or not. Activity of TiO_2 under UVA radiations (20 min) (■) is measured and compared with that measured in the dark (■) and with the bare glass (negative control). Data reported here are the mean values of three replicates +/- standard deviation. Means with different lowercase letters differ significantly ($p<0.05$).

Figure 5. Variation of log reduction of adherent cells onto TiO_2 coatings after UVA activation versus TiO_2 thickness. TiO_2 phase indication on the figure associates the XRD results. (●) *L. monocytogenes ScottA*; (●) *L. monocytogenes ECL136*.

Figure 6. SEM observations (×5 000) of adherent cells of *L. monocytogenes* strains. *L. monocytogenes* ScottA (A, B, C, D) and *L. monocytogenes* ECL136 (E, F, G, H) onto bare glass substrates in the dark (A, E); TiO_2-240nm in the dark (B, F); bare glass substrates after 20 min of UVA illumination (C, G); TiO_2-240nm after 20 min of UVA illumination (D, H).

Figure 7. Absorbance spectra of the MB solution coming from the surface of the various coupons after 60 min of UVA illumination. (A) Bare glass substrate. (B) TiO_2-240nm. MB solution (0.002%) MB solution (0.002%) with mannitol (300 mM).

.

Accepted Article

Table 1. Deposition parameters and characteristics of the TiO_2 thin films.

Layer ID	*Deposition time (min)*	*Substrate temperature (°C)*	*O_2/Ar ratio (%)*	*Thickness d (nm)*	*Crystalline phase*	*Band gap EG (eV)*	*Photocatalytic activity (% of MB discoloration after 60 min of UVA illumination)*
TiO_2-80nm	*60*	*440*	*3*	*80*	*Anatase*	*3.30*	*23.2*
TiO_2-170nm	*120*	*440*	*3*	*170*	*Anatase*	*3.25*	*36.6*
TiO_2-240nm	*180*	*440*	*3*	*240*	*Anatase*	*3.30*	*50.4*
TiO_2-310nm	*240*	*440*	*3*	*310*	*Anatase/Rutile*	*3.25*	*64.1*
TiO_2-400nm	*300*	*440*	*3*	*400*	*Anatase/Rutile*	*3.15*	*89.1*
TiO_2-480nm	*360*	*440*	*3*	*480*	*Anatase/Rutile*	*3.20*	*87.1*

.

Accepted Article

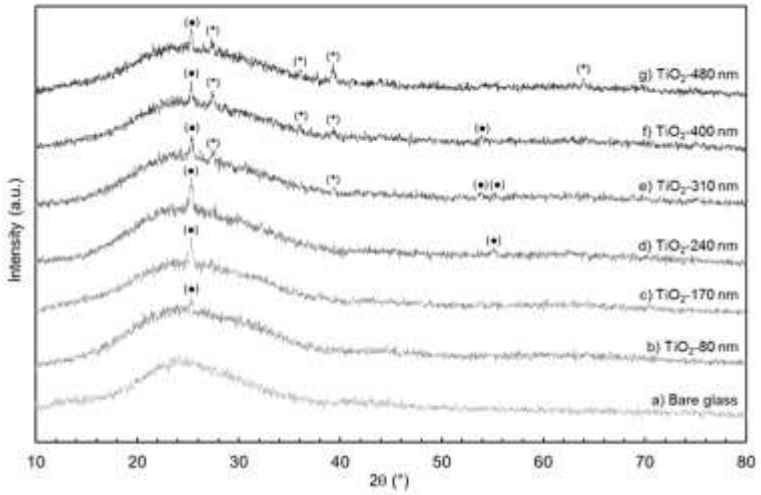

Accepted Article

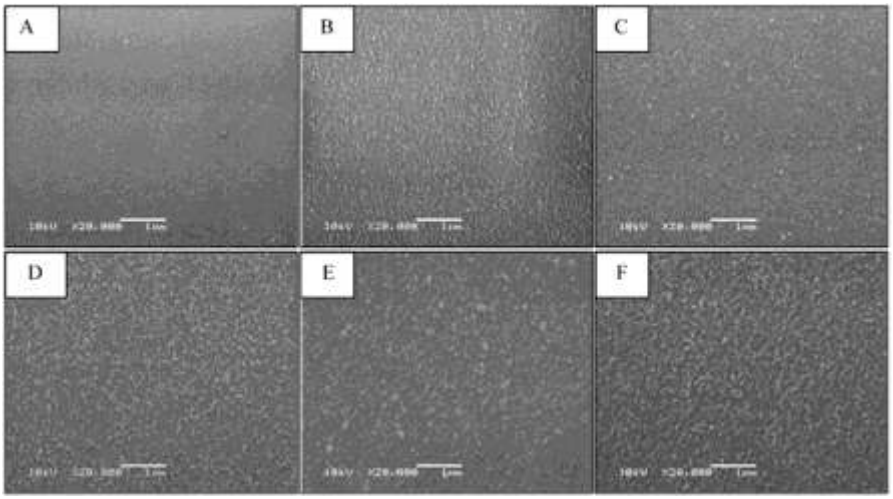

Accepted Article

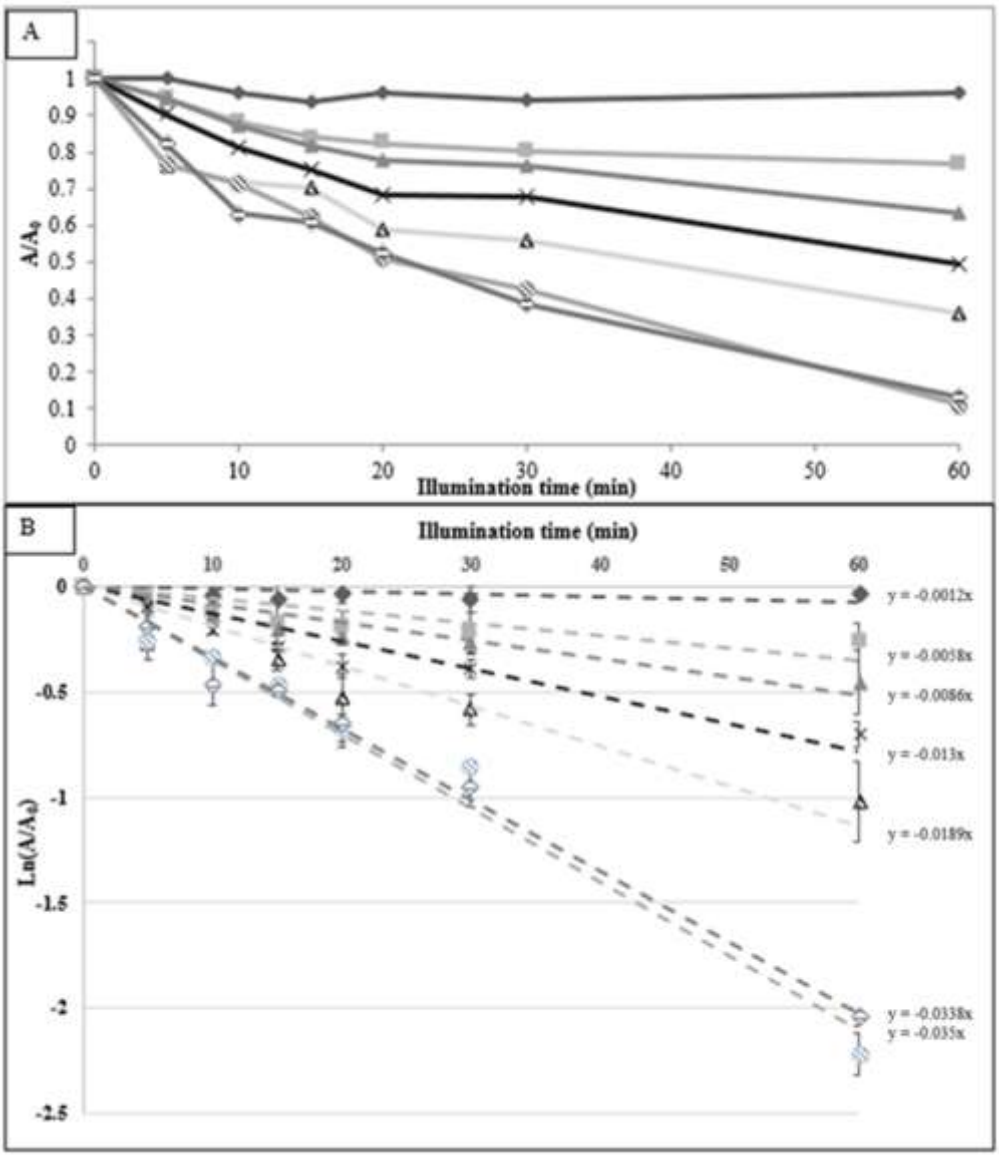

Accepted Article

Accepted Article

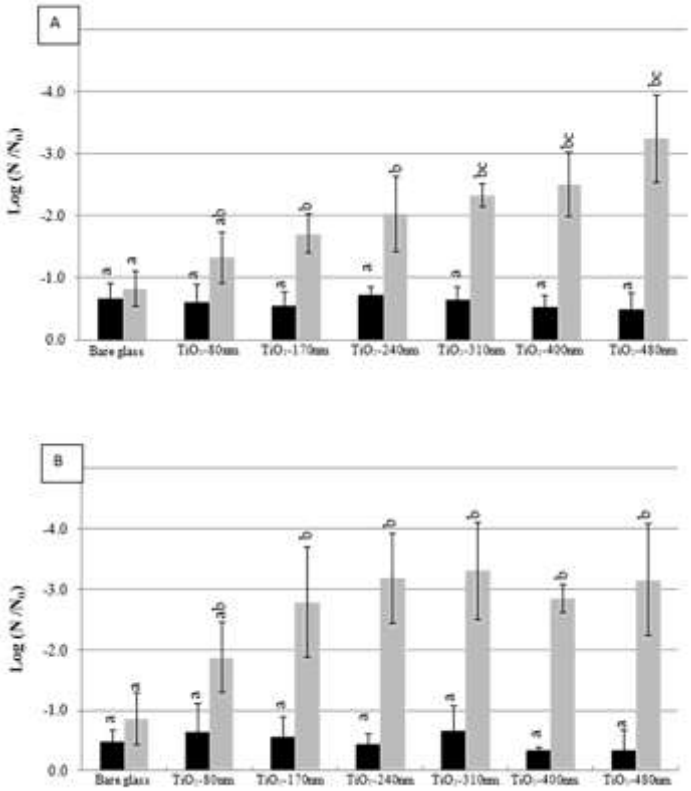

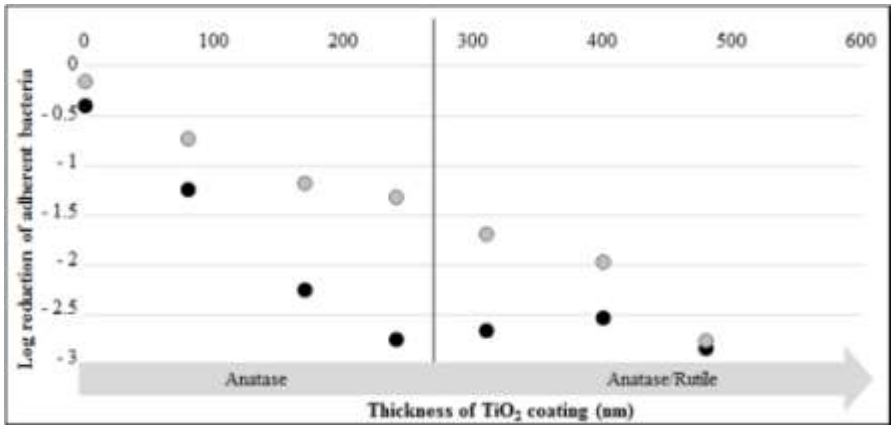

Accepted Article

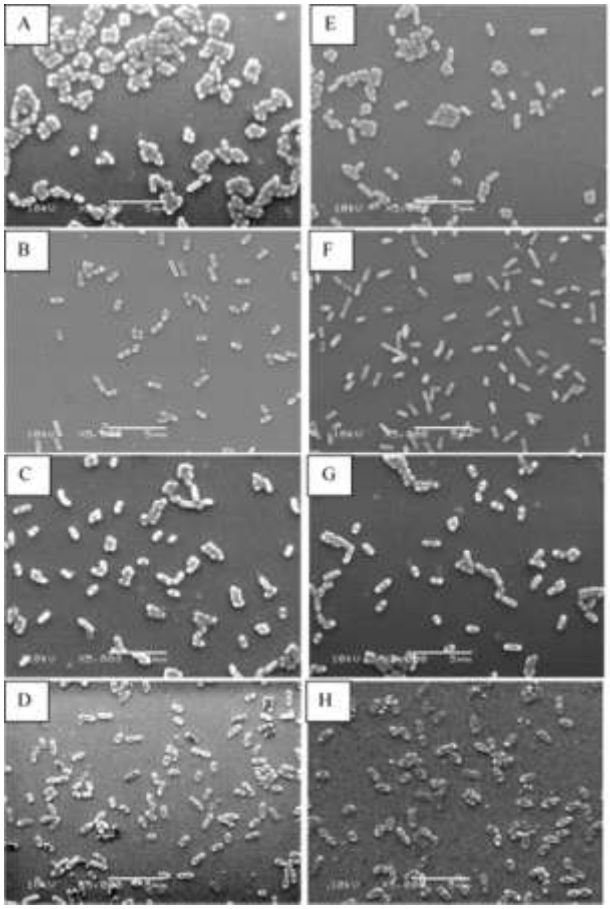

Accepted Article

.

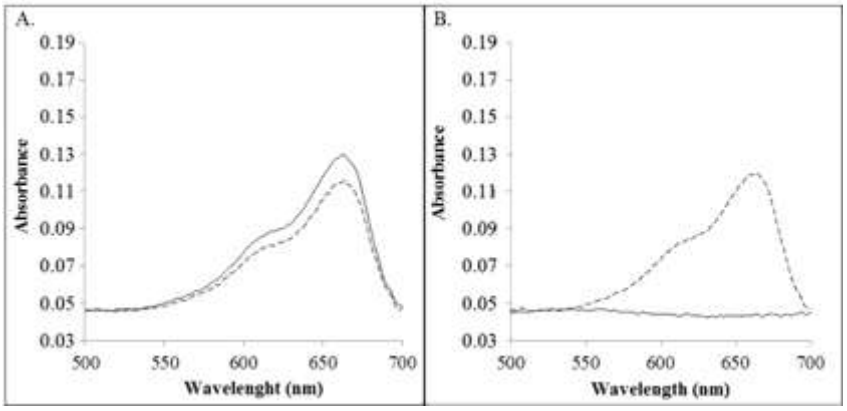

Accepted Article